Applied Surface Science 257 (2011) 4973–4977

Contents lists available at ScienceDirect

Applied Surface Science

journal homepage: www.elsevier.com/locate/apsusc

Growth, modulation and photoresponse characteristics of vertically aligned ZnO nanowires

J.P. Kar[a,b], S.N. Das[a], J.H. Choi[a], T.I. Lee[a], J. Seo[c], T. Lee[c], J.M. Myoung[a,*]

[a] Information and Electronic Materials Research Laboratory, Department of Materials Science and Engineering, Yonsei University, 134 Shinchon Dong, Seoul 120 749, Republic of Korea
[b] Department of Electronics Engineering, University of Tor Vergata, Via del Politecnico, 1-0013 Rome, Italy
[c] Nanobio Device Laboratory, School of Electrical and Electronic Engineering, Yonsei University, 134 Shinchon-Dong, Seoul 120-749, Republic of Korea

ARTICLE INFO

Article history:
Received 6 August 2010
Received in revised form
17 November 2010
Accepted 31 December 2010
Available online 6 January 2011

PACS:
81.05.Dz
81.07.−b
81.15.Gh
78.67.−n
85.60.Gz

Keywords:
ZnO nanowires
Metal organic chemical vapor deposition
Thin film
Etching
Microcavity
Photoresponse

ABSTRACT

Vertically aligned, *c*-axis oriented zinc oxide (ZnO) nanowires were grown on Si substrate by metal organic chemical vapor deposition (MOCVD) technique, where sputtered aluminum nitride (AlN) film was used as an intermediate layer and thermally evaporated barium fluoride (BaF_2) film as a sacrificial layer. The aspect ratio and density of the nanowires were also varied using only Si microcavity without any interfacial or sacrificial layer. The UV detectors inside the microcavity have shown the higher on–off current ratio and fast photoresponse characteristics. The photoresponse characteristics were significantly varied with the aspect ratio and the density of nanowires.

© 2011 Elsevier B.V. All rights reserved.

1. Introduction

In recent years, a great attention has been paid to ZnO nanowires (NWs) because of its wide bandgap (3.4 eV) and a large exciton binding energy (60 meV) with high crystalline quality [1,2]. ZnO NW-based sensors, electronic and optoelectronic devices have already been undertaken due to their excellent material properties, portable size and high surface-to-volume ratio [3,4]. The performance of these devices greatly depends on the quality, aspect ratio, alignment and density of the NWs. However, the characteristics of the NWs can be controlled during their growth and post-deposition processing. The techniques like vapor solid liquid (VLS), metal-organic chemical vapor deposition (MOCVD) and hydrothermal process have already been implemented in order to synthesize ZnO NWs [5–7]. Among these techniques, MOCVD method suits well for the catalytic-free growth of vertically aligned long NWs of good quality.

The most suitable (less lattice misfits) substrates for ZnO growth are $ScAlMgO_4$ and sapphire, which are expensive and technologically incompatible as the fabrication and monolithic integration of semiconductor devices mostly follows CMOS compatible process by adopting Si substrates [8]. On the other hand, large lattice misfits between ZnO NWs and Si substrate deteriorate the quality of the NWs. Hence, the use of an appropriate buffer layer is an alternative process for the growth of well-aligned NWs on Si substrate. Nevertheless, not only the growth, but also the density control of NWs is also required for the successful fabrication of many semiconductor devices. But, low temperature stability and the use of hazardous etchants limit the use of conventional sacrificial layers for the patterning of ZnO NWs by MOCVD techniques. Therefore, an introduction of a novel sacrificial layer for the patterning of ZnO NWs is utmost important. It has also been reported that a patterned (porous) Si substrate modulated the morphology of ZnO nanorods [9]. In order to control both aspect ratio and density, regularly

* Corresponding author. Tel.: +82 2 2123 2843; fax: +82 2 365 2680.
E-mail address: jmmyoung@yonsei.ac.kr (J.M. Myoung).

0169-4332/$ – see front matter © 2011 Elsevier B.V. All rights reserved.
doi:10.1016/j.apsusc.2010.12.158

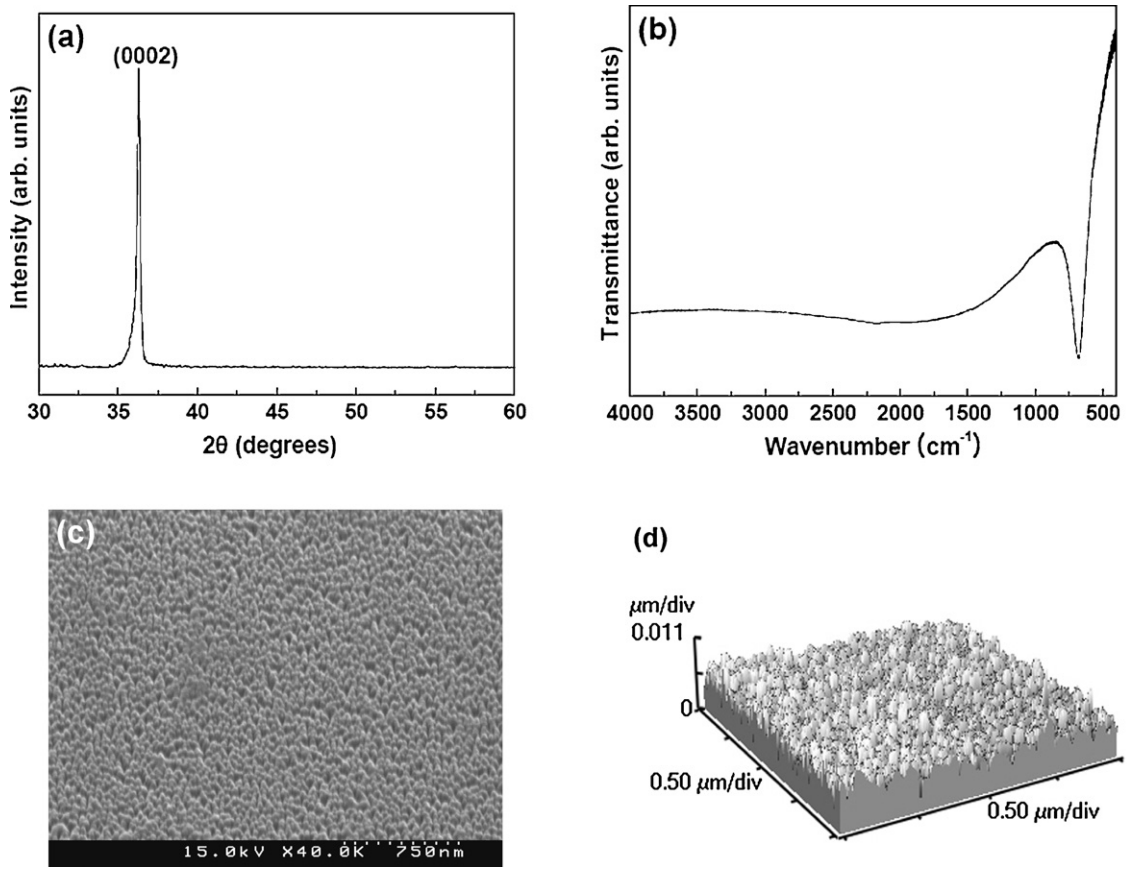

Fig. 1. (a) XRD pattern, (b) FTIR spectrum, (c) SEM, and (d) AFM images of sputtered AlN film.

patterned substrates may also be an alternative option. Furthermore, the fabrication of sophisticated devices, inside the patterned Si microcavity, has the advantages like ease of encapsulation and longevity [10].

Herein, we have studied the effects of buffer layer (AlN), sacrificial layer (BaF_2), and patterned substrates (Si) on the morphology of ZnO NWs. Finally, photoresponse characteristics of the NWs having various aspect ratio and density were investigated through the time-resolved electrical measurements.

2. Experimental

Vertically aligned ZnO NWs were grown by MOCVD method on Si <1 0 0> substrate. Diethyl-zinc (DEZn) and oxygen (5N) were used as the Zn and O_2 sources, respectively. The details of the growth parameters have been reported elsewhere [11]. The interfacial layer (AlN film) was grown by RF magnetron sputtering technique, whereas the sacrificial layer (BaF_2) was deposited by thermal evaporation. AlN film was deposited by RF reactive magnetron sputtering using a pure aluminum target and a mixture of argon and nitrogen gases. The detail growth parameter is reported elsewhere [12]. In a separate experiment, microcavities on the surface of the Si substrate were prepared by micromachining process, where anisotropic etching of Si in selected area was carried out by potassium hydroxide (KOH) solution at 80 °C with 200 nm silicon nitride as masking layer. Then, ZnO NWs were grown at identical deposition conditions by using above mentioned 3-type of substrates. Afterwards, the micrographs of various structures were recorded by field-emission scanning electron microscopy (FESEM, Hitachi S-4200). X-ray diffraction (XRD) studies were carried out using Rigaku (DMAX-2500H) system. Fourier transform infrared (FTIR) spectroscopy (Perkin Elmer, Spectrum BX) was employed for the bond information of AlN film; whereas surface roughness was studied with contact mode atomic force microscope (AFM, Thermomicroscope, CP research system). UV detectors were fabricated on the ZnO NWs grown both outside and inside the microcavity using sputtered Au/Ti films as electrodes, where the inter-electrode spacing and the photosensitive area were defined as 1 mm and 0.3 mm^2, respectively. Time-resolved current (at 3 V) was measured with UV (352 nm) exposure using a semiconductor parameter analyzer (HP4145B).

3. Results and discussion

3.1. Effect of AlN film

Aluminum nitride (AlN) film (500 nm) was sputtered on Si substrate prior to NWs deposition. Fig. 1(a) shows a prominent XRD peak around 36.1°, which depicts the sputtered films are (0 0 0 2) oriented. A FTIR absorption peak at 682 cm^{-1} is observed (Fig. 1(b)), which corresponds to the existence of Al–N bond. Fig. 3(c) and (d) shows a homogeneous growth of AlN films (average grain size ~50 nm) on Si substrate with a RMS roughness of 2 nm. The electrical properties of the AlN film were evaluated from C–V measurements, where the dielectric constant of the film was estimated as 7.1. In addition, the insulator charge density and the interface charge density of the AlN film were found to be 2.2×10^{11} cm^{-2} and 7.6×10^{11} eV^{-1} cm^{-2}, respectively [12].

Fig. 2 shows a typical FESEM image of ZnO NWs grown on AlN/Si. The length and the width of the NWs were found to be around 3–4 μm and 80 nm, respectively. The NWs grown with identical conditions on Si substrate (not shown here) had the lower aspect

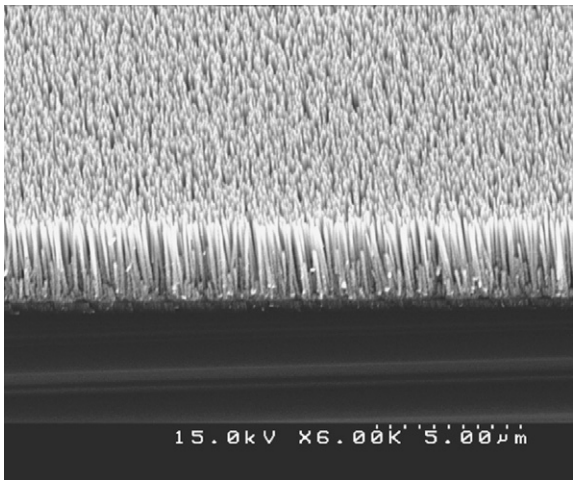

Fig. 2. FESEM image of ZnO NWs grown on AlN/Si substrate.

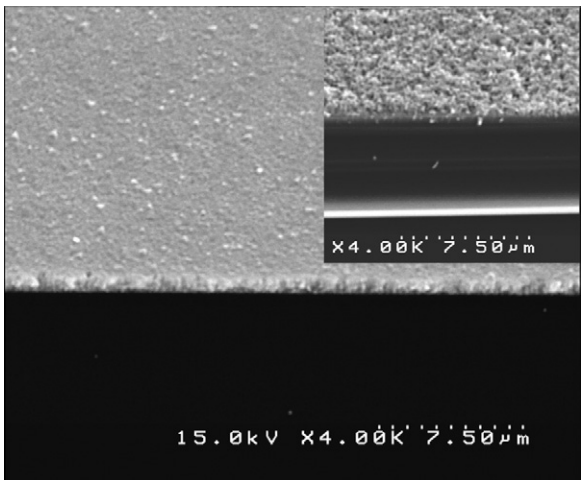

Fig. 3. FESEM images of as-deposited and etched (inset) BaF_2 films.

ratio. The aspect ratio of NWs on AlN/Si substrates was comparable to that of the NWs grown on sapphire substrates [13]. Lower lattice mismatch and the compressive stress in underlying AlN film may be attributed to the formation of ZnO NWs of higher aspect ratio in comparison to bare Si substrates.

3.2. Effect of BaF_2 film

In a separate experiment, thermally evaporated barium fluoride (BaF_2) films were used as a sacrificial layer for micropatterning of ZnO NWs by lift-off method. Here, BaF_2 film has been selected due to its high temperature stability and solubility in deionized (DI) water [14]. Fig. 3 depicts the morphology of as-deposited BaF_2 films. The film was polycrystalline with the RMS roughness of 21 nm. The inset of Fig. 3 shows the modulated surface of BaF_2 films after putting in DI water for 5 min. A nonuniform rough surface was observed as a result of etching. It may be due to the fast etching of defective and porous regions of the film. The etch rate of BaF_2 film was estimated to be around 50 nm/min. This process does not evolve any bubbles, which is a major advantage for the fabrication of low-dimensional devices with sophisticated designs.

Selective growth of the NWs was made by the following techniques. At first, positive photoresist was patterned on the substrate using standard photolithography technique. Thereafter, BaF_2 film (850 nm) was globally deposited on the patterned substrate by thermal evaporation. In order to pattern BaF_2 film, lift-off technique was implemented by removing photoresist in acetone at room temperature. Afterwards, ZnO NWs were globally grown on the patterned BaF_2 film by MOCVD technique at 630 °C. The final step is the etching of BaF_2 film by DI water, where unwanted NWs along with BaF_2 films were selectively removed from the surface of the substrate. In this method, there is a very little chance of the deformation of the NWs since the etching process is free from any hazardous chemicals and hence this method is user friendly. Fig. 4 depicts (a) patterned BaF_2 film, (b) ZnO nanowires growth, and (c) removal of BaF_2 in DI water. The circular patterns (diameter

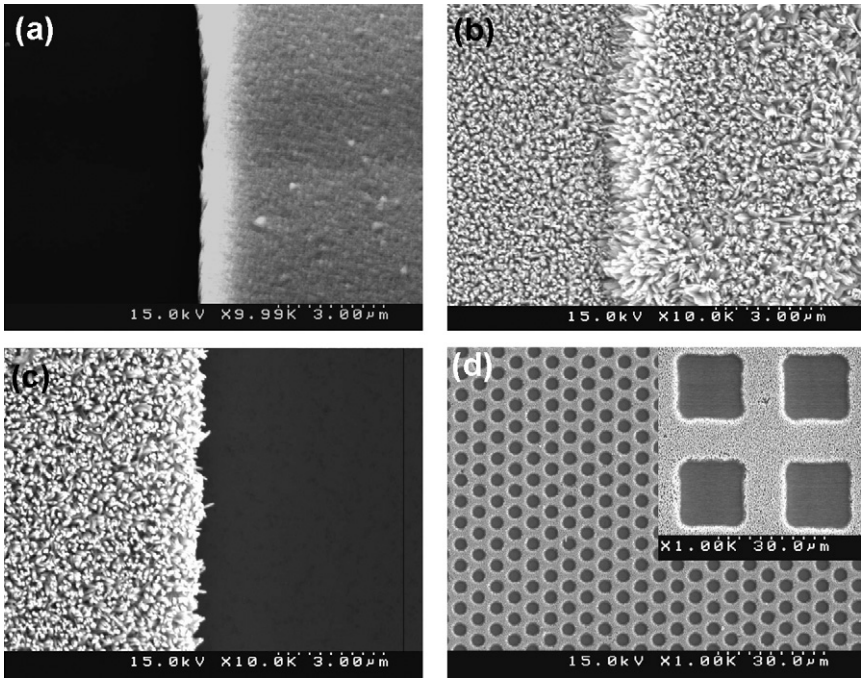

Fig. 4. (a) Patterned BaF_2 film, (b) ZnO NW growth, (c) removal of BaF_2 film in DI water, and (d) circular and square (inset) patterns inside the array of ZnO NWs.

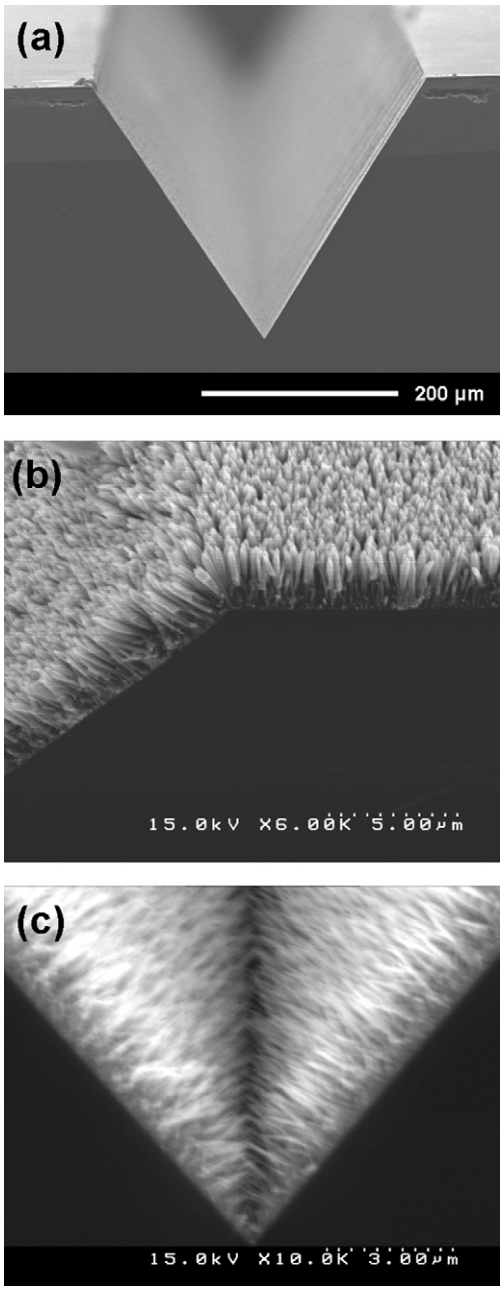

Fig. 5. Cross-sectional SEM images of (a) Si microcavity, (b) ZnO NWs at the top corner of microcavity, and (c) on the bottom inclined surface of the microcavity.

of 3 μm) in ZnO NWs arrays are shown in Fig. 4(d). The inset of Fig. 4 (d) shows square patterns, where the regular periphery is clearly distinguishable. Similarly, the density of the NWs may be controlled by etching of thin BaF_2 layer using sophisticated lithography process.

3.3. Effect of Si microcavity

Chemically (KOH) etched V-shaped Si microcavity is shown in Fig. 5(a). Aqueous solution of KOH attacks Si preferentially in the <1 0 0> plane during etching and produces a characteristic anisotropic V-trench, with sidewalls that form a 54.7° angle with the surface. Then, these patterned Si substrates have been used for the synthesis of ZnO nanowires by MOCVD method. In MOCVD process, ZnO nanowires grow when sufficient compressive in-plane stress develops. This can be achieved by supplying relatively small

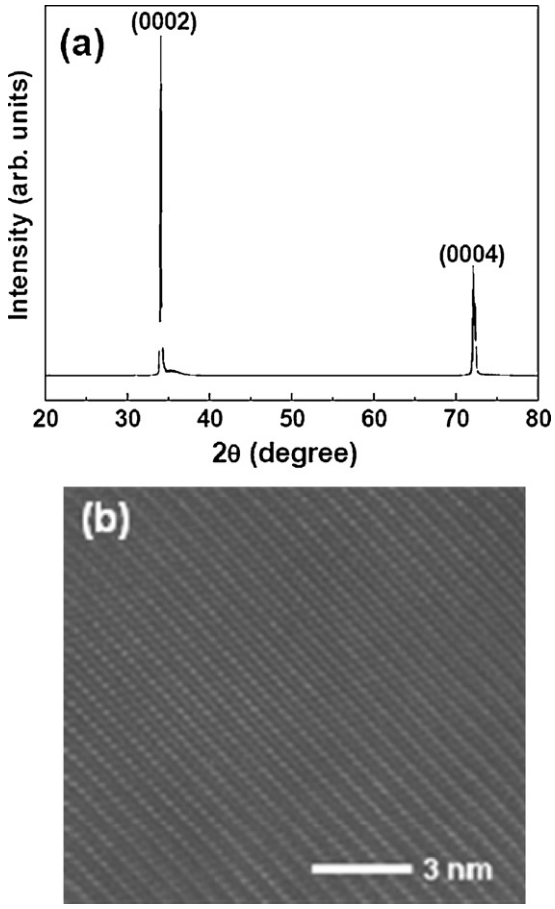

Fig. 6. (a) XRD pattern and (b) HRTEM image of ZnO NWs.

amount DEZn at higher growth temperature. The NWs growth mechanism consists of two stages: nucleation and growth. At first, nanosized crystalline nuclei are formed on the substrate surface and afterwards *c*-axis oriented vertical ZnO NWs are grown due to the fastest growth rate along (0 0 0 2) direction. The anisotropic growth of ZnO NWs is explained by considering the supersaturation and surface diffusion phenomena, which can be controlled by changing both the growth parameters and the nature of the substrates [6,13]. The aspect ratio and the number density of NWs outside the cavity (Fig. 5(b)) were around 10 and 10^7 per mm^2, respectively. Fig. 5(c) shows the cross-sectional SEM image of the ZnO NWs at the bottom inclined surfaces of the microcavity. The NWs grown inside the microcavity have an aspect ratio and number density of 20 and 5×10^7 per mm^2, respectively. Hence, both the aspect ratio and the density of NWs can be varied using patterned substrates without any interfacial or sacrificial layer. At the inclined surface of the cavity, the growth direction (*c*-axis) and the direction of incoming precursor molecules are not same. Also, during the growth, the gaseous species become stagnant due to the unavailability of fresh precursor molecules inside the microcavity. So, the width of NWs was less than those grown outside the cavity. Also, NWs of higher aspect ratio have less chance of the coalescence inside the cavity. Furthermore, the sharpness of the NWs in the cavity may be due to the lack of reactant supply during the growth [15].

3.4. Photoresponse of the ZnO nanowires

From the above experimental results, it is clear that the aspect ratio and the density of nanowires can be varied by using *c*-axis

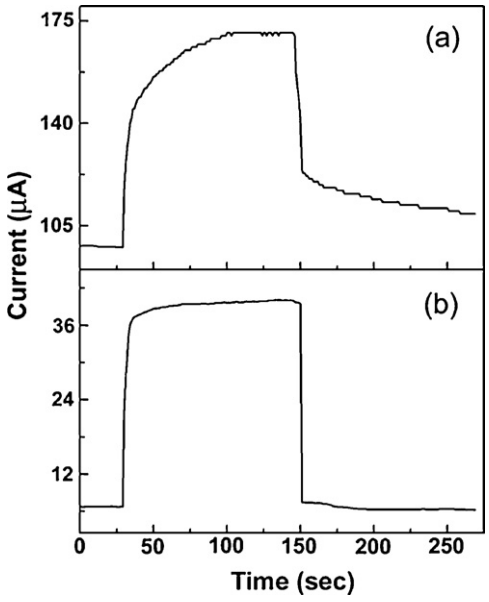

Fig. 7. Time-resolved photoresponse of ZnO NWs based UV detectors fabricated on (a) outside and (b) inside of the Si microcavity.

oriented AlN film and BaF_2 layer, which require complicated processes and become cost effective. But one can easily synthesize NWs with controlled density and high aspect ratio by using Si microcavity as a substrate. Hence, ZnO NW-based UV photodetectors were fabricated both in and outside of the microcavity, where one can get NW arrays of variable aspect ratio and the density in a single growth by MOCVD without using AlN and BaF_2 films. Before the fabrication of UV detectors, the structural properties of the ZnO NWs were investigated. The preferential growth of the NWs is along (0 0 0 2), as observed from XRD patterns (Fig. 6(a)). High-resolution transmission electron microscopic (HRTEM) image of ZnO NW is shown in Fig. 6(b). The inter-planar spacing is estimated as 0.52 nm, which corresponds to (0 0 0 1) orientation of ZnO NWs. The results, obtained from structural investigations, depict the growth of ZnO NWs are along *c*-axis. The NWs are single crystalline, structurally uniform and do not exhibit any noticeable defects. A clean, atomically sharp and smooth surface was also observed without any sheathed amorphous phase.

After the fabrication of UV detectors, time-resolved variation of current is measured at a constant voltage (3 V) with UV exposure plotted in Fig. 7(a) and (b) for NWs outside and inside of the microcavity, respectively. Similar results were observed after performing several on–off cycles. The NWs fabricated inside the microcavity have shown fast UV response. Initially, a lower base line dark current was observed, which may be due to the trapping of free electrons at the surface of the NWs by the adsorption of atmospheric oxygen. The adsorbed oxygen, present at the surface of NWs, acts as shallow trapping centers and forms a surface depletion layer, which reduces the conductivity of the NWs. When the energy of the exposed UV light is more than the bandgap of ZnO, the current increased rapidly to a certain level and then gradually became saturated. During UV exposure, a large number of electron-hole pairs are created at the surface [16]. The photogenerated holes recombine with the chemisorbed oxygen ions on the surface. At the same time, the electrons contribute to the conduction. After turning off the UV light, the free electrons at the surface reduces by adsorbing oxygen and decrease in conductance has been observed. The symbolic representation of the UV response characteristic can be expressed as;

$$O_{2(g)} + e^- \rightarrow O^-_{2(ad)} \quad (1)$$

$$h\nu \rightarrow e^- + h^+ \quad (2)$$

$$O^-_{2(ad)} + h^+ \rightarrow O_{2(g)} \quad (3)$$

The photo/dark current (on/off) ratios of the UV detectors fabricated out and inside of the microcavity were calculated as 1.8 and 6, respectively. The higher on/off ratio may be due to the higher surface-to-volume ratio of NWs grown in the microcavity. The current has come back to its initial state after turning off the UV light. The decay times of the UV detectors fabricated outside and inside the microcavity were around 100 s and 5 s, respectively. This may be due to the fast recombination of photogenerated electron-hole pairs due to the adsorption of oxygen at the NWs surfaces inside the microcavity. The photoresponse characteristics can be further improved by functionalizing the surface and increasing surface to volume ratio of NWs [17–19].

4. Conclusion

The enhancement in aspect ratio and the patterning of the vertical aligned ZnO NWs were carried out using AlN and BaF_2 films as interfacial layers. On the other hand, both the aspect ratio and density of the NWs were varied by using anisotropically etched patterned Si substrate without any interfacial layer. Morphological and structural studies confirmed the single crystalline growth of the ZnO NWs along (0 0 0 2) orientation. NWs, grown inside the microcavity, have shown better UV response with base line recovery at dark condition. The photoresponse characteristics were significantly varied with the aspect ratio and the density of NWs. These approaches can promote the versatile use of ZnO NWs for next generation of electronic devices.

Acknowledgement

This work was supported by the IT R&D program of MKE/IITA [2008-F-023-01] and WCU (World Class University) program through the National Research Foundation of Korea funded by the Ministry of Education, Science and Technology [R32-20031].

References

[1] Y.W. Heo, D.P. Norton, L.C. Tien, Y. Kwon, B.S. Kang, F. Ren, S.J. Pearton, J.R. Laroche, Mater. Sci. Eng. R 47 (2004) 1.
[2] Z.L. Wang, Mater. Today 7 (2004) 26.
[3] J.G. Lu, P. Chang, Z. Fan, Mater. Sci. Eng. R 52 (2006) 49.
[4] Z.L. Wang, Mater. Sci. Eng. R 64 (2009) 33.
[5] H.C. Hsu, C.S. Cheng, C.C. Chang, S. Yang, C.S. Chang, W.F. Hsieh, Nanotechnology 16 (2005) 297.
[6] M.C. Jeong, B.Y. Oh, W. Lee, J.M. Myoung, J. Crystal Growth 268 (2004) 149.
[7] L. Vayssieres, Adv. Mater. 15 (2003) 464.
[8] A. Ievtushenko, V. Karpyna, G. Lashkarev, V. Lazorenko, V. Baturin, A. Karpenko, M. Lunika, A. Dan'ko, Acta Phys. Polon. A 114 (2008) 1131.
[9] J.P. Kar, M.H. Ham, S.W. Lee, J.M. Myoung, Appl. Surf. Sci. 255 (2009) 4087.
[10] P. Pal, S. Chandra, Smart Mater. Struct. 13 (2004) 1424.
[11] J.P. Kar, M. Kumar, J.H. Choi, S.N. Das, S.Y. Choi, J.M. Myoung, Solid State Commun. 149 (2009) 1337.
[12] J.P. Kar, G. Bose, S. Tuli, Mater. Sci. Semicond. Process 8 (2005) 646.
[13] J.P. Kar, S.W. Lee, W. Lee, J.M. Myoung, Appl. Surf. Sci. 254 (2008) 6677.
[14] S. Mukherjee, S. Jain, F. Zhao, J.P. Kar, D. Li, Z. Shi, Microelectron. Eng. 85 (2008) 665.
[15] S. Lee, A. Umar, S.H. Kim, N.K. Reddy, Y.B. Hahn, Korean J. Chem. Eng. 24 (2007) 1084.
[16] Y. Li, F.D. Valle, M. Simonnet, I. Yamada, J.J. Delaunay, Nanotechnology 20 (2009) 045501.
[17] C.S. Lao, M.C. Park, Q. Kuang, Y. Deng, A.K. Sood, D.L. Polla, Z.L. Wang, J. Am. Chem. Soc. 129 (2007) 12096.
[18] Y.W. Heo, B.S. Kang, L.C. Tien, D.P. Norton, F. Ren, J.R. La Roche, S.J. Pearton, Appl. Phys. A 80 (2005) 497.
[19] A. Bera, D. Basak, Appl. Phys. Lett. 93 (2008) 053102.